Forest Volume and Biomass Estimation Using Small-Footprint Lidar-Distributional Parameters on a Per-Segment Basis

Jan A.N. van Aardt, Randolph H. Wynne, and Richard G. Oderwald

Abstract: This study assessed a lidar-based, object-oriented (segmentation) approach to forest volume and aboveground biomass modeling. The study area in the Piedmont physiographic region of Virginia is composed of temperate coniferous, deciduous, and mixed stands. Segmentation objects, hierarchical in terms of area and ranging from 0.035 to 5.632 ha/object, were created using a lidar-derived canopy height model. Horizontal point (basal area) samples were used to calculate volume and aboveground biomass. Per-object lidar point (per return height and intensity) distributional parameters were extracted from small-footprint lidar. Adjusted R^2 and Mallow's Cp metrics were used to select models for the range of segmentation results. Selected variables included intensity-based and structurally related first through fifth return height parameters. Object-based modeling (adjusted $R^2 = 0.58–0.79$; various object sizes) resulted in distinct improvements over stand-based attempts (adjusted $R^2 = 0.40–0.73$; majority adjusted $R^2 < 0.50$). Adjusted R^2 and RMSE values for deciduous volume (0.59; 51.15 m^3/ha) and biomass (0.58; 37.41 Mg/ha) were better than those found for another, plot-based study in the study area. Coniferous R^2 values for volume (0.66) and biomass (0.59) were lower than previous studies, which was attributed to variability within the relatively narrow volume range (6.94–50.93 m^3/ha). FOR. SCI. 52(6):636–649.

Key Words: Multiresolution, segmentation, remote sensing, laser altimetry.

F OREST VOLUME AND BIOMASS have long been estimated using extensive in-field inventory methods or aerial photography volume tables (Avery and Burkhart 1994). Although field-based methods are typically unbiased, both approaches are time-consuming and expensive. Digital, large-scale remote sensing could provide a less expensive option for estimation of forest biophysical parameters over large tracts, while potentially also providing accurate and unbiased estimates. The structural nature of lidar height data makes it especially suitable for gauging forest volume and biomass. Lidar-based forest measurements are not only of importance to general forest inventory and canopy structure modeling (Lefsky et al. 2002a, b, Næsset 2002, Popescu et al. 2004), but also to estimation of forest fuel loads (Riaño et al. 2003, Seielstad and Queen 2003) and derivation of digital elevation models (DEMs) (Popescu et al. 2002, Hodgson et al., 2003), all topics applicable to forest management and site mapping. Lefsky et al. (2002a) stated that lidar sensors are able to provide accurate and nonasymptotic estimates of various forest indices such as LAI and aboveground biomass. Lidar systems, furthermore, could reduce the need for ground-based, small scale measurements of tree heights and/or canopy parameters, and provide increased automation and positional accuracy compared to photogrammetric techniques.

Large-footprint lidar sensors have been used extensively for forest volume and biomass estimation (Lefsky et al. 1999, Means et al. 1999, Lefsky et al. 2002b). These sensors typically have ground footprints of 5 to 25 m diameter (Lefsky et al. 1999), as opposed to small-footprint sensors with sub-meter diameter footprints, e.g., 0.65 m, used in this study. The size of the footprint, coupled with typically low horizontal sampling densities, limits the applicability of large-footprint lidar sensors at the scale of active forest management. However, small-footprint lidar measurements, typically with multiple samples per square meter, enable users to estimate volume and biomass even for small tracts of forest. Small-footprint sensors have been used as early as the mid-1980s for forest volume estimation (Maclean and Krabill 1986, Nelson et al. 1988). Small-footprint lidar-volume studies have implemented both plot- and stand-based approaches (Nilsson 1996, Popescu et al. 2004). Lidar height distributional approaches, based on extraction of height distributional parameters (e.g., median, mode, percentiles) from all lidar returns within spatial units such as grid cells, also have come to the fore (Means et al. 2000, Næsset 2002). A lidar distributional approach to forest volume and biomass modeling lends itself to object or stand level application. Although they are not, strictly speaking, waveforms, these distributions do have some similarities to

J.A.N. van Aardt, CSIR–Natural Resources and the Environment–Ecosystems, PO Box 395, Pretoria 0001, South Africa—jvaardt@csir.co.za. Randolph H. Wynne, Department of Forestry, Virginia Polytechnic Institute and State University, 319 Cheatham Hall, Blacksburg, VA 24060—wynne@vt.edu. Richard G. Oderwald, Department of Forestry, Virginia Polytechnic Institute and State University, 138 Cheatham Hall, Blacksburg, VA 24060—oderwald@vt.edu.

waveforms since all height returns are accumulated per sampling unit, resulting in per-unit height-frequency distributions with high vertical resolution due to integration over large objects. Like waveforms, these distributions enable the characterization of canopy vertical structure, useful for fine-scale, stand-level forest volume and biomass estimation (Magnussen and Boudewyn 1998, Means et al. 2000, Drake et al. 2002, Lefsky et al. 2002b, Næsset 2002).

Magnussen and Boudewyn (1998) illustrated that the distribution of canopy heights for a Douglas-fir (*Pseudotsuga menziesii*) stand was a function of vertical distribution of foliage area. The proportion of laser pulses returned from a given height was proportional to the fraction of leaf area above it. This relationship was used to estimate mean stand height and a strong correlation ($R^2 = 0.8$; SD = 2.2 m) was found between laser and field estimates. Such a result corroborated the usefulness of a distributional approach in characterizing vertical structure. Means et al. (2000) implemented a lidar distributional approach to estimate height and basal area for Douglas-fir stands, ranging from shrublike (18 m^3/ha) to old-growth (1,313–2,051 m^3/ha) stands. Lidar returns were extracted from 10 × 10 m grid cells within larger 50 × 50 m measured plots. Distributional parameters, e.g., canopy cover percentiles, maximum height, elevation, average mean height, and average of the maximum heights, were calculated for grid cells. Stepwise regression analysis was used to determine the relationships between ground data and lidar measurements, with dependent variables being height, basal area, and volume. R^2 values of 0.93 (RMSE = 3.4 m), 0.95, and 0.97 (no RMSE for the latter two values) were obtained for height, basal area, and volume, respectively. R^2 values for plots excluding old-growth plots were 0.98 (RMSE = 1.7 m), 0.94 (RMSE = 5.4 m^2/ha), and 0.95 (RMSE = 73 m^3/ha), for height, basal area, and volume, respectively. Various percentile variables, e.g., the 90th height percentile and 20th coverage percentile, were shown to be significant predictor variables. Næsset (2002) predicted volume and crown parameters for Norway spruce (*Picea abies*) and Scots pine (*Pinus sylvestris*) stands in Norway, using a stratum-specific (young forests; old-growth, on poor and good sites) approach. Observed volume values ranged between 41 m^3/ha and 639.8 m^3/ha. Lidar first and last pulse distribution-based regression equations were used to model volume and crown parameters. Various quantiles, maximum and mean values, canopy density measures, and coefficients of variation were used as independent variables. R^2 values for 61 reference stands were 0.87 (dominant height) and 0.91 (volume). Standard deviations ranged between 0.7 and 1.33 m (dominant height) and 18.3 and 31.9 m^3/ha (volume).

Extension of distributional grid-cell approaches, i.e., where lidar data are extracted per square sampling unit, to object- and stand-level applications was a logical next step. An object refers to a spatial entity that is homogenous in terms of a selected property, as opposed to continuous fields (Burrough and McDonnel 1998). Segmentation output can be treated as entities or objects, since each object is homogenous in terms of a defined variable. Such an application requires that distinct forest cover and structural types have different, unique lidar canopy densities or distributions (Douglas et al. 2003), and that object-level data have the potential to decrease associated object-level errors (Makela and Pekkarinen 2001, Pekkarinen 2002). Object-based modeling not only extends a grid- or plot-level approach, but also is amenable to stand-level scaling, since objects can match existing structural management boundaries in forests. However, scaling efforts assume that objects are hierarchical and topologically sound, i.e., smaller-level objects are exact constituents of larger-level objects.

The basic precept of this study was that extraction of lidar distributions on a grid-cell basis, used to model volume and biomass (Means et al. 2000, Næsset 2002), could be extended to estimation at the object or forest stand level. The specific objective of this study was to determine whether volume and aboveground biomass can be estimated successfully using object-oriented analysis of lidar distributions. The success Means et al. (2000) and Næsset (2002) had with their cell-based distributional approaches boded well for the methodology in this study, since they showed that heights, basal area, and volume can be estimated for coniferous species using cell-derived distributions. Object-based modeling extends this approach to estimate biophysical parameters for discrete entities derived from the lidar data themselves.

Methods
Study Area

The 946 ha (2,338 acre) study area is located in Appomattox Buckingham State Forest (Appomattox County) in the Piedmont physiographic province of Virginia, southeastern USA, at 78°41′W, 37°25′N (Figure 1). The mean elevation of the study area is 185 m (606 ft), with minimum and maximum elevations of 133 m (436 ft) and 225 m (738 ft), respectively. Local topography can best be described as gentle rolling slopes and flat terrain. Vegetation is composed of various coniferous (*Pinus taeda*, *P. virginiana*, *P. echinata*, and *P. strobus*), deciduous (*Quercus coccinea*, *Q. alba*, and *Liriodendron tulipifera*), and mixed forests.

Available Data

Lidar data were acquired by Spectrum Mapping, LLC using the DATIS II (small-footprint, high-density, multiple return) system. The lidar data were acquired on Sept. 9, 2002, centered at 78°40′30″W, 37°25′9″N, and covered an area of approximately 958 ha (2,367 acres). Specifications of the lidar data set are given in Table 1.

Field data consisted of 256 mapped basal area plots (BAF; basal area factor 10) on a 16 columns by 16 rows, 201.17 m (10 chains) grid spacing. Field data were collected during the summer, fall, and winter months (May–Dec.) of 2003. Differentially corrected plot location, plot basal area and diameter at breast height (dbh), height, and species were determined for all plots and tallied trees. A total of 219 BAF
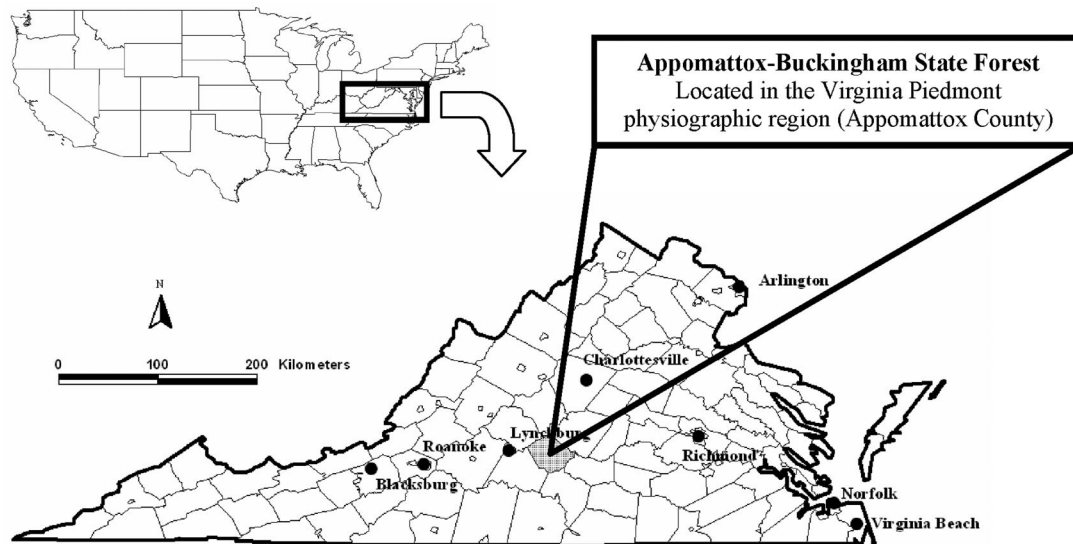
Figure 1. Study area: Appomattox Buckingham State Forest, Virginia, USA.

Table 1. DATIS II lidar data set characteristics

Characteristic	Specifications
Laser altitude	2,000 m (6,562 ft.) above ground level
Laser scan field-of-view	75° maximum
Swath width and centerline spacing	800 m (2,625 ft.) and 400 m (1,312 ft.)
Scan rate	25 Hz
Laser pulse rate	35 kHz
Scan angle	± 13.5°
Returns	≤ 5
Resolvable distance between returns	0.75 m
Footprint	0.46 m (1.51 ft.)
Spacing across/along track	1 m (3.3 ft.)/2 m (6.6 ft.)
Accuracy (X, Y, Z)	X, Y: 0.5 m; Z: 0.15 m (X, Y: < 1.6 ft.; Z: < 0.49 ft.)
Post-processed GPS accuracy	< 0.05 m
Wavelength	1,064 nm

plots ultimately were used in the statistical analysis since 37 plots were located on private land or had basal area values of zero (no forest type differentiation possible).

Plots were assigned to two- and three-class forest type schemes based on basal area percentages. "Deciduous" or "Coniferous" types were defined as plots that had 50% or greater basal area contribution, i.e., majority contribution, from either deciduous or coniferous species, respectively. A "Mixed" class was added to the three-class type designation for plots that had less than 90% basal area contribution for either deciduous or coniferous species. A 90% cutoff was based on final sample numbers for the two- and three-class schemes. The two-class analysis consisted of 140 deciduous and 79 coniferous plots, while the three-class analysis consisted of 112 deciduous, 56 coniferous, and 51 mixed plots. This allowed for volume and biomass model development based on adequate plot samples (>30) for both the two- and

three-class analysis. Only 25 (11.4%) of the plots were mixed when a 75% cutoff was used, resulting in a redundant class that was too small for viable statistical analysis.

The BAF plots were expanded to a per-hectare basis for each object, since per-object field plot data were used for model development and validation. This was done using standard BAF expansion equations (Avery and Burkhart 1994).

Volume and biomass equations (Saucier and Clark 1985, Clark et al. 1986, Schroeder et al. 1997, Sharma and Oderwald 2001) for per-tree calculations were similar to the equations used by Popescu et al. (2004). This latter study was situated within the same geographical boundaries, with the same species being studied. Specific volume and biomass equations were used for loblolly and other southern pines, as well as for hardwoods. Volume and biomass were calculated on an individual tree basis for each plot and expanded to per-hectare values for each object. Plots were assigned to the object in which they were located. This was done through poststratification for selected segmentation results. BAF plot values were averaged on a per-object basis in the case of larger objects that contained more than one field plot. Descriptive statistics for all basal area plots are given in Table 2.

Lidar Data Processing

A canopy height model (CHM) was needed for segmentation. Seven outliers (>6 m difference from neighboring values), attributed to "bird-hits" or lidar error, were removed. The first returns were median-filtered by 1-m grid cells to remove per-cell values that were redundant to subsequent interpolation procedures. Bare ground returns were supplied by the data provider and were based on a proprietary algorithm that incorporates the return number and associated intensity to identify nonvegetation last returns. First-order canopy returns and ground returns, i.e., vegetation-removed last returns, were interpolated to a 1-m spatial

Table 2. General descriptive information for deciduous, coniferous, and mixed plots

Class and Type	Parameter	Minimum	Maximum	Average	σ
2-class					
Deciduous plots (140)	Volume/ha (m^3/ha)	6.94	350.65	157.64	84.14
	Biomass/ha (Mg/ha)	11.11	269.01	113.60	58.60
	Basal area/ha (m^2/ha)	2.30	34.44	16.32	7.84
Coniferous plots (79)	Volume/ha (m^3/ha)	8.32	350.93	114.49	75.44
	Biomass/ha (Mg/ha)	4.67	155.56	41.47	26.64
	Basal area/ha (m^2/ha)	2.30	36.73	14.24	7.91
3-class					
Deciduous plots (112)	Volume/ha (m^3/ha)	6.94	350.65	156.16	89.32
	Biomass/ha (Mg/ha)	11.11	269.01	117.31	62.53
	Basal area/ha (m^2/ha)	2.30	34.44	15.97	8.21
Coniferous plots (56)	Volume/ha (m^3/ha)	8.32	278.99	100.45	66.42
	Biomass/ha (Mg/ha)	4.67	81.65	33.66	19.95
	Basal area/ha (m^2/ha)	2.30	36.73	13.61	8.11
Mixed plots (51)	Volume/ha (m^3/ha)	31.68	350.93	156.85	72.60
	Biomass/ha (Mg/ha)	20.06	175.75	81.49	38.93
	Basal area/ha (m^2/ha)	4.59	36.73	16.84	6.68

resolution grid using regular Kriging, since Popescu et al. (2002) found this to be the most accurate interpolation technique using similar data for the same study area. This approach effectively addressed instances where a 1-m grid cell lacked an original input value. The resultant 1-m resolution was detailed enough to detect road and stand breaks in the segmentation process. Interpolation was performed using Surfer 7.0 software (Golden Software, Inc.). The differenced first- and ground return surface (CHM) was used as input to the eCognition segmentation algorithm. This allowed for extraction of forest objects based on height homogeneity and distinct stand breaks, e.g., roads and slope breaks.

The distributional modeling approach, based on height distributional parameters, required that lidar data be processed on a per-return basis to retain information related to the return hierarchy. Ground hits were removed using Terrascan V. 003.002 (Terrasolid, Inc.) and MicroStation V. 08.00.04.01 (Bentley Systems, Inc.) software. This algorithm identifies ground hits based on iterative slope analysis of lidar returns. *Grid cell size* and *maximum slope of the area* are required input parameters. Grid cell size is the smallest cell size for which a ground return can be extracted. A cell size of 10 m was used to extract a maximum number of ground returns for the first (31,294,660), second (11,101,215), and third (2,121,989) returns. Grid cell sizes of 39 m and 119 m were used for the fourth (175,093) and fifth (5,379) returns, respectively. Larger grid cell sizes were required for the last two categories due to the small number of returns in each case. These latter two cell sizes occurred in cases where the number of ground hits reached a maximum for the fourth and fifth returns as algorithm cell size was increased. This approach was based on the assumption that most of the hits from the fourth and fifth return categories would be ground hits due their ranking in the return hierarchy. A slope percentage parameter of 35% was used as a maximum for the area, obtained from a USGS DEM. Ground returns constitute an important component of

overall lidar distributional patterns and were retained as data sets on a per-return basis.

Nonground hits, designated as vegetation hits, were normalized for varying terrain elevations, thereby enabling volume and biomass models to incorporate actual lidar point heights (Means et al. 2000). This was done by calculating the actual return height above a lidar-derived 1-m DEM of the study area. The actual height of each vegetation hit was calculated as the difference between the vegetation hit and the bilinear interpolated height of the four corner cells of the DEM cell directly beneath each hit, using Surfer V. 8.1 software (Golden Software, Inc.).

Segmentation of the Study Area

Segmentation was performed using a multiresolution, hierarchical algorithm (eCognition V. 3.0; Definiens imaging 2003) applied to the lidar-derived CHM of the study area. Lidar data were considered a structural component, ideally suited to defining homogenous structural objects through segmentation. The eCognition algorithm considers an entire image, evaluates object homogeneity (within-object variance), shape, compactness, and smoothness, and expands objects across the image to ensure resultant objects of similar size and shape (Baatz and Schäpe 2000). This algorithm requires color:shape and smoothness:compactness ratios as input parameters. The color:shape ratio was set at 0.8:0.2, based on the recommendation of the developers (Baatz and Schäpe 2000, eCognition 2003) and evaluation of alternative parameter inputs. Object smoothness was considered more important than shape in a forestry context, since smooth, boundary-following objects are preferable to compact, blocky objects. The smoothness:compactness weight combination therefore also was set at 0.8:0.2.

Although eCognition was chosen as the preferred segmentation approach, one could argue that the segmentation method is subordinate to the utility that resultant objects

have to analyses. Even though a multitude of segmentation approaches exist in literature, e.g., the Woodcock-Harward (centroid linkage) algorithm (Shandley et al. 1996), a Hough transform-based approach (Shankar et al. 1998), and watershed-based hierarchical segmentation (Li et al. 1999), it is ultimately of great importance that segmentation results are robust. Other important factors are ease of operational use, widespread availability, and adequate software support. eCognition, furthermore, was the preferred approach for segmentation because of its hierarchical nature, correspondence to input data, and since results from this algorithm have been validated in the natural resources context (Kayitakire et al. 2002, Nugroho et al. 2002a, b, Engdahl et al. 2003, Kellndorfer and Ulaby 2003, Kressler et al. 2003).

The decision of which segmentation results to use for model development was based on between- and within-object variability of the CHM: Models were fitted to segmentation results where within-object variability was smaller than between-object variability. The smallest selected object size corresponded to the circular BAF plot area, with radii defined by average tallied tree distance from BAF plot centers plus one and two standard deviations. This ensured that objects were representative of plot-level field data, based on corresponding areas. Ten average object sizes, ranging from 0.035 ha/object to 3.942 ha/object, subsequently were chosen for volume and biomass model development. This was done to evaluate model performance across a range of average object sizes. The current Appomattox stand map (167 stands, 5.666 ha/stand) also was selected, as well as the segmentation result that corresponded to the number of operational stands (168 objects, 5.632 ha/object). Operational stands were used to compare object-based modeling to stand-based modeling. Vegetation and ground lidar data sets were extracted on a per-object basis for all segmentation results using ARCGIS V. 8.3 software (ESRI). Resultant data sets were exported to SAS V. 8.02 software (Level 02M0; SAS, Inc.) for subsequent regression analysis.

Regression Analysis

The intent of this study was to extend lidar distributional, grid-cell forest volume and biomass modeling (Means et al. 2000, Næsset 2002) to estimation at the object or forest stand level. Lidar distributions should be representative of stand structural characteristics such as canopy closure and stand height distribution. Theoretically, distributions from whole objects approximate waveform lidar data for that object, which in turn gives an indication of vertical vegetation distribution, a property closely related to biomass (Magnussen and Boudewyn 1998, Means et al. 2000, Næsset 2002). Intermediate return distributions also had potential utility, since these returns represent forest structure. A multi-tiered forest structure theoretically will have many intermediate returns, while an even-aged, weed-controlled, and thinned pine stand might exhibit a majority of first and last returns, with few intermediate hits.

Distributional parameters were derived only for first- and second-return vegetation data sets because of objects with missing parameter values for the third through fifth returns. An object with limited or sparse vegetation, for instance, potentially could exhibit only first and last returns due to sparser understory or reduced canopy complexity, while cursory analysis showed that all objects had at least two sets of returns. Distributional parameters included the mean, coefficient of variation, kurtosis, maximum, minimum, mode, range, standard error of the mean, skewness, SD, number of observations, height percentile points at 10% intervals of height values, and canopy cover percentiles. Canopy cover percentiles were based on the proportion of first returns smaller than a given percentage, in steps of 10%, of maximum height to include all possible first-return values. For example, the 10% canopy cover percentile was defined as the ratio of per-object first returns smaller than 10% of the maximum height and the total number of first returns for that object. The ratio of the number of vegetation or ground hits and the total number of lidar hits per object also was calculated. This was done for the second and third through fifth group vegetation hits, as well as first, second, and third through fifth group ground hits. The vegetation ratio for each object was calculated as the ratio of the number of vegetation hits per object and the total hits for that object. These distribution metrics have been shown to be useful descriptors of tree volume for 10×10 m grid cells in Douglas-fir, western Oregon stands (Means et al. 2000) and 200 m^2 sample plots in Norway spruce and Scots pine stands in southeast Norway (Næsset 2002). Lidar intensity distributional parameter values for the first and second returns included the intensity mean, median, coefficient of variation, maximum, minimum, range, standard error of the mean, and SD.

Linear regression analysis was performed using object volume and biomass as dependent variables. Independent variables were reduced by a forward selection process with α values set between 0.075 and 0.350 as significance levels for remaining in the model. The goal was to reduce independent variables from 75 initial variables to fewer than 10 variables in all cases. Forward selection was chosen over the stepwise selection used by Means et al. (2000), since forward selection retains all significant predictor variables, whereas stepwise selection discards variables that become less significant as more variables are added. Variables were validated based on Pearson's correlation coefficients between independent and dependent variables. All variables with correlations of 0.8 or lower were retained. However, only the variable with the highest correlation to the dependent variable was retained in cases where independent variable correlations were higher than 0.8, thereby ensuring an objective variable selection. A value of 0.8 was chosen based on data characteristics, with the knowledge that all lidar-derived variables are height-related, resulting in inherently high correlations. This cutoff value resulted in predictive variables remaining in developed models, while highly correlated variables ($r > 0.9$) were eliminated. These methods were crucial to avoid statistically invalid models

(overfitting) in the final regression step, namely linear regression using Mallow's Cp and adjusted R^2 as selection criteria.

Mallow's Cp selection takes all combinations of independent variables into account while calculating a value related to the mean square error of a fitted value for all models (Draper and Smith 1981, Montgomery et al. 2001). Approximately 10 or fewer candidate models from many recombination possibilities were selected for each model based on Mallow's Cp and adjusted R^2 values, as well as number of independent variables. Although Mallow's Cp and adjusted R^2 values alone were valid fit criteria, RMSE (where applicable), model simplicity and model validity also were considered. Cases with a very slight increase in Cp values (<1 unit) and decrease in adjusted R^2 values (~0.01), with the benefit of fewer independent variables, were considered simpler with marginal sacrifice in fit statistics. Lastly, models with less abstract independent variables, e.g., range, mean, and maximum values, were favored over models with variables related to standard error of the mean, coefficient of variation, SD, and the like.

Regression analyses were performed for segmentation results of 0.035 ha/object, 0.091 ha/object, 0.141 ha/object, 0.318 ha/object, 0.642 ha/object, 0.964 ha/object, 1.263 ha/object, 1.885 ha/object, 2.53 ha/object, 3.942 ha/object, 5.632 ha/object, and the Appomattox Forest stands (5.666 ha/object). Analyses were applied to two- and three-class schemes as well as for all objects combined. In the first case, models were fitted to the Deciduous and Coniferous groups. Deciduous objects numbered from 61 to 140 objects, while coniferous objects ranged between 34 and 79 objects, depending on the average object size and number of BAF plots that were averaged for larger object sizes. Analyses were performed on Deciduous (43–112 objects), Coniferous (22–56 objects), and Mixed (30–51 objects) classes in the case of the three-class forest scheme. Regression analyses were limited to objects with nonmissing values for distributional parameters used in Mallow's Cp regression selection. The only case with missing distributional parameter values occurred at 0.035 ha/object (27,050 objects) for the two-class (16/140 deciduous and 9/79 coniferous missing objects) and three-class (14/112 deciduous and 1/51 mixed missing objects) forest definitions.

Results

Variable reduction through implementation of forward selection succeeded in reducing independent variables from the original 75 variables to fewer than 10 in each case. Variables were well distributed across the entire range of possible selections, with no evident trend in variable selection. Distributional variables were present for vegetation hits from the first and second returns, while intensity variables, percentiles, canopy cover percentiles, and ratio variables all were represented across forest types and segmentation treatments. Intensity mean, maximum, and range variables of both first- and second-return vegetation hits were especially well represented. This indicated that intensity values are of significance in the modeling of forest biophysical parameters (Means et al. 1999, Brandtberg et al. 2003). Kurtosis and skewness variables were prevalent in deciduous and coniferous volume and biomass variable sets. Although vegetation or canopy cover percentiles often were well represented, only the percentile most highly correlated to the dependent variable ultimately was selected. Specific significant variables, related to a forest type, were frequently present in both the volume and biomass models for that type. This was not unexpected due to volume and biomass being highly correlated metrics ($r \approx 0.87$). Strong representation from a wide range of distributional parameters indicated that simple metrics such as mean and extreme values were supplemented by parameters such as skewness, kurtosis, percentiles, and canopy percentiles. Results such as these build a strong case for the use of multiple return lidar data, and even associated intensity-per-return, for the modeling of forest biophysical parameters. This might be especially critical in areas that contain forests with high variability in site, growth, and composition. The inclusion of second-return variables indicates that forest structure is an important aspect in volume and biomass modeling approaches. Second-return variables, by definition, contribute to defining height levels other than the upper to top canopy, describing aspects of forest vertical structure besides canopy height.

Lidar height distributions were found to be representative of BAF plot measurements. Figure 2 shows the lidar first-return vegetation distributions for randomly selected deciduous and coniferous objects across a range of volume-per-hectare field measurements. Objects with lower measured volume-per-hectare exhibited either fewer hits at taller tree heights or generally shorter trees than objects with higher volume-per-hectare measurements. Changes in distribution types also were evident with distributions for lower volume-per-hectare objects being skewed to the right, and vice versa. Distributions for intermediate volume-per-hectare objects resembled normal distributions. Model selection of percentile, skewness, canopy cover, and kurtosis variables were evident when distributions were evaluated. Factors such as skewness and percentage hits below percentiles were logical selections for distinguishing between different volume-per-hectare levels, based on distribution shapes and height frequencies. Metrics such as minimum and mean values also played a role due to the number of returns at the lower and upper limits of each distribution and their contribution to the measured minimum and average value.

Figure 3 shows an example of deciduous and coniferous objects with similar volume-per-hectare values across increasing average object sizes. Distributions for each type visually remained similar in shape as average object size increased. Coniferous distributions, for example, remained relatively similar in shape as average object size increased, although the number of returns increased, resulting in a smoother curve. There were no distinct trends visible when deciduous were compared to coniferous distributions, although there appeared to be more upper and lower tail
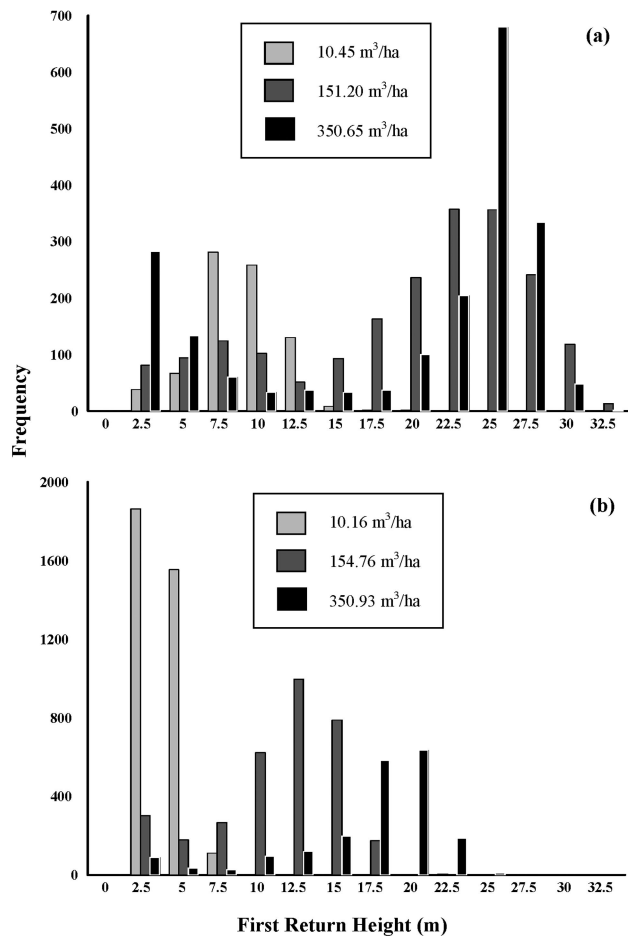
Figure 2. (a) Deciduous and (b) coniferous per-object (0.035 ha/object) histogram plots for lidar first-return vegetation hits across a range of field-measured volume-per-hectare.
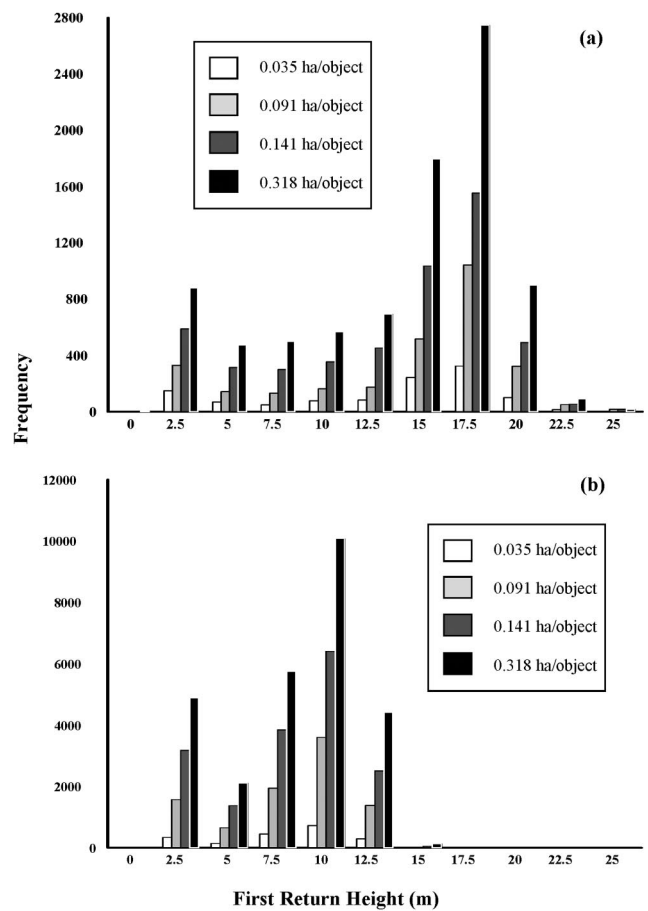

Figure 3. (a) Deciduous and (b) coniferous first-return, vegetation height distributions for variable size objects with 153.02 m³/ha and 159.50 m³/ha volume, respectively.

values in the case of deciduous objects. This was attributed to trees of above-average height and undergrowth, respectively, as commonly found in an uneven-aged stand.

Correlation analysis formed a critical component of the preprocessing analysis by removing unwanted high correlations, reducing independent variables even further, and ensuring viable, valid models. Correlated variables were intuitive in most cases, e.g., the 20th, 30th, and 50th first-return vegetation percentiles. However, thorough evaluation of variable correlations was required to identify other highly correlated variables, e.g., the 70th percentile of the first returns and the 30th canopy cover percentile. Percentile metrics especially were problematic in terms of correlations. Two-thirds of percentile parameters often had to be removed due to high inter-variable correlations. Table 3 lists final variable sets that were used as input to Mallow's Cp selection, after significance and correlation reduction, and that ultimately resulted in the best adjusted R^2 values for all forest types. Variables again were distributed across the entire spectrum of possibilities, with canopy cover and regular percentiles well represented, and even intensity values still being present. Mallow's Cp selection, which followed variable reduction, resulted in an exhaustive combina-

tion-set of independent variables, with model Cp values increasing and adjusted R^2 values decreasing as model complexity increased.

Table 4 lists the best-performing models (adjusted R^2) and associated descriptive statistics for two- and three-class forest schemes, as well as the adjusted R^2 and RMSE values for the existing Appomattox stands (5.666 ha/object). Figures 4 and 5 show the residual behavior for the best performing two-class volume and biomass models, 5.632 ha/object and 0.091 ha/object, respectively. Final model selection was based on Cp, adjusted R^2, RMSE, and especially number of independent variables. The latter criterion was crucial due to the close performance of candidate models based on other fit statistics. Except for coniferous volume and biomass models, most models could be limited to five or fewer independent variables without appreciable loss in goodness-of-fit for each specific forest type. This was attributed to the relative homogeneity found in such coniferous stands, resulting in an increased number of independent variables that were correlated to the dependent variables, as opposed to heterogeneous deciduous stands, where fewer independent variables were deemed significant for modeling (Figures 2 and 3). Pure forest stands in public ownership are relatively limited in the Virginia Piedmont, resulting in variable mixed stands with basal area

Table 3. Final variable sets that were used as input to Mallow's Cp selection, after significance and correlation reduction, and ultimately resulted in the best adjusted R^2 values for all forest types selection

Model	Variables	Removed variables	Adjusted R^2	Object size (ha)
2-class Volume				
D	P_Veg2_10 P_Veg2_70 MinInt2 ZeroNgrnd3_5ratio Canopy20P Canopy80P	SkewnessVeg2 SkewnessVeg1	0.59	5.632
C	ModeVeg1 P_Veg1_40 RangeVeg2 MedianVeg2 StdInt2 ZeroNgrnd3_5ratio	Canopy30P	0.66	5.632
A	CVVeg1 MinVeg1 P_Veg1_50 MaxInt1 MedianInt1 MinVeg2 Canopy30P	P_Veg1_70	0.59	0.091
2-class Biomass				
D	MinVeg1 P_Veg2_10 P_Veg2_75 CVInt2 ZeroNVeg2ratio Canopy20P Canopy70P	KurtosisVeg2 Canopy80P	0.58	5.632
C	CVVeg1 P_Veg1_20 MedianInt1 P_Veg2_40 StdInt2 Vegratio Canopy40P Canopy70P	None	0.59	0.091
A	CVInt1 CVVeg2 P_Veg2_10 P_Veg2_30 P_Veg2_75 ZeroNVeg3_5ratio Canopy80P	P_Veg1_30	0.66	5.632
3-class Volume				
D	MinInt1 MaxVeg2 ModeVeg2 P_Veg2_70 ZeroNgrnd3_5ratio	CVVeg2 MinInt2	0.62	5.632
C	P_Veg1_30 StdMeanInt2 StdInt2 MedianInt2 ZeroNgrnd1ratio Canopy70P	None	0.67	0.642
M	ModeVeg1 MinInt1 MinVeg2 StdMeanInt2 ZeroNgrnd1ratio Canopy10P Canopy50P Canopy80P	None	0.74	5.632
3-class Biomass				
D	ModeVeg2 P_Veg2_75 RangeInt2 StdMeanInt2 ZeroNgrnd3_5ratio Canopy90P	KurtosisVeg2 MinInt2	0.62	5.632
C	P_Veg1_25 MedianInt1 StdInt2 MedianInt2 ZeroNgrnd3_5ratio	None	0.63	3.942
M	KurtosisVeg1 MinVeg1 ModeVeg1 P_Veg1_10 CVInt1 RangeInt1 ZeroNVeg3_5ratio Canopy60P Canopy80P	Canopy50P	0.79	5.632

D = deciduous; C = coniferous; A = all objects/types; M = mixed.

Veg = Vegetation lidar hit; Grnd = Ground lidar hit; Int = Intensity associated with lidar hit; Veg1, 2, or 3_5 = first, second, or grouped third through fifth returns; P_...._10–90 = Percentiles; CV = Coefficient of variation; StdMean = Standard error of the mean; Std = Standard deviation; Canopy10–90 = Canopy cover percentiles; N...ratio = Vegetation or ground hits as a ratio of return totals; Vegratio = Vegetation hits as a ratio of total hits

contribution from both deciduous and coniferous species. While mixed deciduous stands have similar heterogeneous characteristics, a deciduous-coniferous mix resulted in lower R^2 values when compared to the more homogenous coniferous type.

Discussion

Adjusted R^2 values for coniferous species volume were lower than those found in two comparable studies by Means et al. (2000, adjusted R^2) and Næsset (2002, R^2), both of which used a grid-cell based lidar distribution approach to volume modeling. R^2 values for these two studies ranged from 0.91 to 0.97, while species were limited to Douglas-fir (*Pseudotsuga menziesii*) (Means et al. 2000) and Norway spruce (*Picea abies*) and Scots pine (*Pinus sylvestris*) (Næsset 2002). Stands also varied from shrublike (18 m³/ha) to old-growth (2051 m³/ha) (Means et al. 2000) and young forest (41 m³/ha) to mature forest (639.8 m³/ha) in the case of Næsset (2002). The

Table 4. Models with the highest adjusted R^2 values for volume and biomass modeling for 2- and 3-class schemes

Model	Object adjusted R^2	Stand adjusted R^2	Object RMSE (m^3/ha or Mg/ha)	Stand RMSE (m^3/ha or Mg/ha)	Object size (ha)
2-class Volume					
D: 262.37385 + 19.92957 P_Veg2_70 + 208.14833 ZeroNgrnd3_5ratio −387.67008 Canopy80P	0.59	0.44	51.15	63.56	5.632
C: 458.52340 − 4.18276 ModeVeg1 + 15.43186 P_Veg1_40 − 5.59238 RangeVeg2 − 0.36692 StdInt2	0.66	0.48	38.03	55.61	5.632
A: 309.84855 + 0.29731 CVVeg1 + 13.66277 MinVeg1 + 11.12989 P_Veg1_50 − 0.14246 MedianInt1 − 432.13149 MinVeg2 + 55.39894 Canopy30P	0.59	0.42	53.75	62.36	0.091
2-class Biomass					
D: 271644 + 1,3993 P_Veg2_75 − 286090 ZeroNVeg2ratio −75577 Canopy70P	0.58	0.43	37.41	45.84	5.632
C: 185653 + 2262.86568 P_Veg1_20 − 29.74409 MedianInt1 + 3533.08872 P_Veg2_40 − 91682 Vegratio −20694 Canopy70P	0.59	0.40	17.15	19.45	0.091
A: 343583 −1370.95705 CVInt1 + 316.85290 CVVeg2 + 1,5082 P_Veg2_75 − 132911 ZeroNVeg3_5ratio −314776 Canopy80P	0.66	0.46	33.14	41.18	5.632
3-class Volume					
D: −31.77814 + 19.67658 P_Veg2_70	0.62	0.46	55.98	68.16	5.632
C: 303.72815 + 15.71060 P_Veg1_30 − 1.78646 StdMeanInt2 − 0.59669 StdInt2 + 0.06230 MedianInt2 + 737.63803 ZeroNgrnd1ratio + 146.83730 Canopy70P	0.67	0.73	38.24	40.08	0.642
M: 255.71328 − 3.17225 ModeVeg1 + 1.54155 MinInt1 − 5.84654 StdMeanInt2 − 444.06932 ZeroNgrnd1ratio −111.50951 Canopy10P −145.92581 Canopy50P −413.21393 Canopy80P	0.74	0.57	28.02	46.68	5.632
3-class Biomass					
D: −134083 + 1,6205 P_Veg2_75 + 2460.48834 StdMeanInt2 + 159205 ZeroNgrnd3_5ratio	0.62	0.46	39.48	48.61	5.632
C: −84498 + 6498.76606 P_Veg1_25 + 44.56384 MedianInt1 − 81.96051 StdInt2 + 7,8560 ZeroNgrnd3_5ratio	0.63	0.70	12.06	12.56	3.942
M: 1493940 − 601912 MinVeg1 + 4984.27818 P_Veg1_10 − 370.80540 RangeInt1 + 8,4546 ZeroNVeg3_5ratio −612016 Canopy80P	0.79	0.68	16.32	20.29	5.632

D = deciduous; C = coniferous; A = all objects/types; M = mixed
Veg = Vegetation lidar hit; Grnd = Ground lidar hit; Int = Intensity associated with lidar hit; Veg1, 2, or 3_5 = first, second, or grouped third through fifth returns; P_...._10–90 = Percentiles; CV = Coefficient of variation; StdMean = Standard error of the mean; Std = Standard deviation; Canopy10–90 = Canopy cover percentiles; N . . . ratio = Vegetation or ground hits as a ratio of return totals; Vegratio = Vegetation hits as a ratio of total hits

range of forest volume and growth-types, low single species variability, averaging effect of plot-based measurements, and fixed plot measurements that directly corresponded with lidar plot boundaries could have contributed to higher R^2 values in
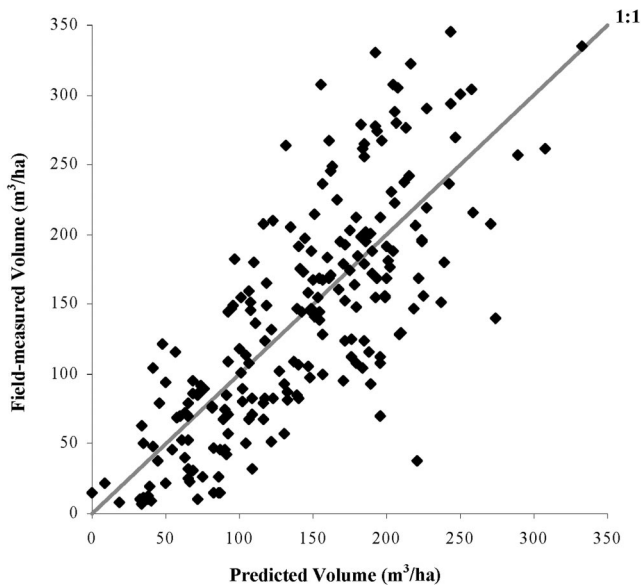
Figure 4. Two-class volume model (0.091 ha/object): Field-measured versus predicted volume/ha values for all plots combined (adjusted $R^2 = 0.59$).
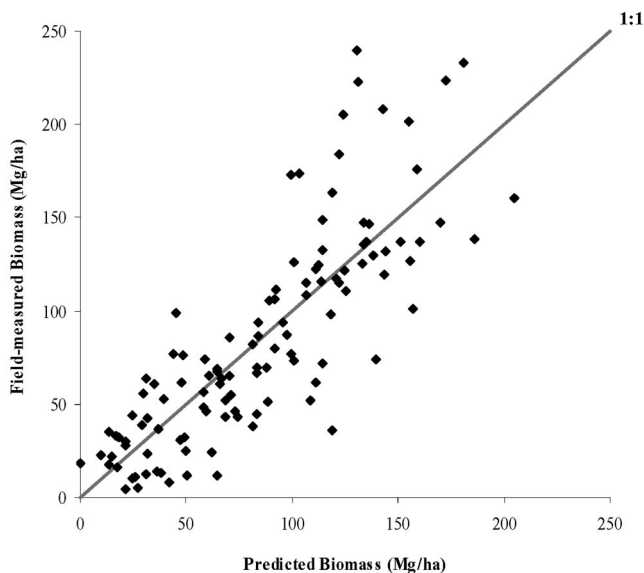

Figure 5. Two-class biomass model (5.632 ha/object): Field-measured versus predicted biomass/ha values and residuals for all plots combined (adjusted $R^2 = 0.66$).

these two studies. However, RMSE values were comparable to those found by Means et al. (2000; 73 m³/ha, old-growth plots excluded) and Næsset (2002; 18.3–31.9 m³/ha), indicating that an object-based approach has potential for extension to operational application.

Coniferous adjusted R^2 values for volume in this study ranged from 0.46 (two-class, 1.885 ha/object) to as high as 0.67 (three-class, 0.642 ha/object. Lower adjusted R^2 values were attributed to a narrower range in volume and biomass-per-hectare values for this study (6.94–350 m³/ha; 4.67–269.01 Mg/ha). This was due to more intrinsic variability found in this narrower range, while an increased

observed range with lower variability likely will result in better model fit statistics. Plot sampling technique also was a potential source of variability. Unlike the complete grid-cell inventory by Means et al. (2000), not every tree within an object was measured in this approach. Although BAF plot measurement is an established forestry inventory technique, it does not account for all trees on a given plot. The assumption that each object was represented by its enclosed BAF plot therefore could have had an impact on the results.

Coniferous RMSE values for this study (38.03–56.73 m³/ha; 12.06–19.70 Mg/ha) compared favorably with those found by Means et al. (2000, 73 m³/ha) and Næsset (2002, 18.3–31.9 m³/ha). This is of practical importance, since model extension to real-world estimates is reliant on precision estimates. Considering the range of deciduous RMSE values from 50.39 m³/ha to 61.72 m³/ha (volume) and 37.41 Mg/ha to 48.61 Mg/ha (biomass), operational applications are feasible. RMSE values are of greater importance to operational implementation than R^2 values since they provide information on the precision of the estimate.

Although coniferous results were worse than those for a plot-level lidar study of Popescu et al. (2004) in the same area, adjusted R^2 values for deciduous types were significantly higher. The highest values for this study were 0.59 (two-class, 5.632 ha/object) and 0.62 (three-class, 5.632 ha/object) versus an unadjusted R^2 of 0.36 found by Popescu et al. (2004). This latter result is of importance, indicating the potential of an object-based approach to deciduous volume- and biomass modeling, specifically when compared to Forest Inventory and Analysis (FIA) type plots. Object-based, as opposed to plot-based, approaches might be better suited to deciduous modeling due to the more diverse structure of deciduous growth being captured through data-derived objects. Small-radius plot-level deciduous volume and biomass modeling are problematic due to extra-plot stand variability and the large size (crown width) of old-growth deciduous trees.

Derivation and use of objects as measurement units encapsulated deciduous units better than a fixed plot-based approach. However, the lower coniferous adjusted R^2 values found in this study were attributed to the relative diversity in coniferous objects. This is in direct comparison to the previous plot-based approach, where a majority of coniferous plots were located within uniform coniferous stands and captured the homogenous nature of such stands without inclusion of more heterogeneous coniferous components, such as stand boundaries. A two-class (deciduous-coniferous) modeling approach furthermore lent itself to inclusion of objects with only marginally more coniferous than deciduous basal area. This in turn resulted in reduced adjusted R^2 values due to increased within-object variability. It should be noted that an n-class modeling approach, where $n > 2$, also has disadvantages. These include smaller object numbers per class, along with reduced feasibility for operational applications due to more complex model fitting requirements. Although a three-class approach therefore has disadvantages when compared to a two-class scheme, there was no definitive difference between two- and three-class

model metrics. Deciduous adjusted R^2 values ranged between 0.51 and 0.59 (two-class) and 0.52 and 0.62 (three-class), while coniferous values ranged between 0.46 and 0.66 (two-class) and 0.47 and 0.67 (three-class). Adjusted R^2 values for the mixed class in the three-class scheme ranged between 0.43 and 0.74. These results indicated that a simpler, two-class approach was well suited to the study area, but that a three-class scheme remains an option to the user, depending on operational implications.

Model fit statistics did not exhibit vast differences among different object sizes, but generally did deteriorate with increasing average object size. Except for the 5.632 ha/object result, with high adjusted R^2 values for coniferous ($R^2 \approx 0.66$), deciduous ($R^2 \approx 0.59$), and combined models ($R^2 \approx 0.54$), the general trend was for fit statistics to become worse with increasing object size. This was true for object sizes between 0.091 ha/object and 3.942 ha/object, with a general decreasing trend in adjusted R^2 values and an increasing trend in RMSE values. A definitive reason for the increase in adjusted R^2 values in the case of 5.632 ha/object was not evident. This increase was attributed to better representation of BAF plot data at the larger object size through inclusion of multiple BAF plots for per-object modeling, while within-object variability remained adequately small to obtain acceptable model fit statistics. Further research is required to definitively address this issue. The lack of distinct differences among average object sizes also is an artifact of the hierarchical segmentation algorithm. Minimization of within-object variance occurred at the smaller average object sizes, while these smaller objects form the building blocks for larger objects. Within-object variance therefore already has been minimized at smaller object size levels, with the hierarchical structure not further contributing to reducing this within-object variance.

Model metrics for the operational Appomattox stands were distinctly lower than those found in the case of segmentation applications for the two-class scheme. Deciduous adjusted R^2 and RMSE values for volume modeling were 0.44 and 63.56 m^3/ha, while values for coniferous stands were 0.48 and 55.61 m^3/ha, respectively. Overall modeling results were 0.42 and 62.36 m^3/ha, which indicated that segmentation has distinct advantages over current defined stands in the study area. These trends are evident in Table 4, with the modeling improvement due to segmentation being attributed to definition of modeling units using the same data source and units having lower within-object variance. Although adjusted R^2 values for three-class coniferous volume ($R^2 \approx 0.73$) and biomass ($R^2 \approx 0.70$) were high relative to other results, this was attributed to the current stand definition being based on homogenous, even-aged coniferous stands. This came at the cost of low adjusted R^2 values for deciduous stands for volume ($R^2 \approx 0.46$) and biomass ($R^2 \approx 0.46$).

Adjusted R^2 was found to be a metric well suited to model evaluation, especially considering a relatively large number of height distribution variables (≤ 7) needed to explain the variability in the dependent variables. Adjusted R^2 values of up to 0.59 (two-class deciduous volume), 0.67

(three-class coniferous volume), and 0.59 (combined volume) were deemed acceptable given the variability associated with public forests in the Virginia Piedmont. Stands often are mixed to a large degree, resulting in large within-stand variation. Adjusted R^2 values for biomass were as high as 0.62 (deciduous), 0.63 (coniferous), and 0.66 (combined). Although no definitive trend was prevalent, adjusted R^2 values were higher while RMSE values were lower in most model cases for smaller average object sizes (0.035–0.318 ha/object) as opposed to larger objects (0.141–5.632 ha/object). Smaller objects have smaller within-object variability with associated higher between-object variance.

Evaluation of residual values for all models confirmed model validity, with no alarming trends in residual values. Although most plotted residuals were evenly distributed around zero, with only a limited number of outliers, a slight increase in residuals with increasing predicted values were detected in some cases (deciduous and combined models). This minor variance heteroskedasticity was attributed to two main factors. Biomass models have been shown to have a "fan-shaped" residual trend with increasing predicted values. This is especially true for predicted biomass values greater than 100 Mg/ha (Parresol 1999). The biomass equations used to model tree biomass were based only on tree diameter, and not on measured height values (Schroeder et al. 1997). This is a common practice (Schroeder et al. 1997, Parresol 1999), but could have contributed to poor residual distributions due to independent variable differences between biomass equations and lidar-based biomass models. Lidar data are inherently height-based data sources, while most biomass models do not include height as an independent variable. Volume and biomass modeling using logarithmic transformations of the dependent and independent variables were attempted, but the heteroskedasticity effect was not substantially reduced.

Conclusions

Grid-cell volume and biomass modeling based on lidar distributions have been implemented successfully by Means et al. (2000) and Næsset (2002). These studies were limited to coniferous species, but R^2 values upward of 0.90 bode well for future lidar distributions studies. This study explored an extension of the grid-cell approach to unique forest objects and a deciduous-coniferous forest mix. Hierarchical, multiresolution segmentation results were used as homogenous units for the extraction of lidar distributions, while basal area plots were used as field data for model fitting and validation. No distinct differences were found for volume and biomass modeling attempts across increasing object sizes (0.035–5.632 ha/object), although adjusted R^2 values generally decreased and RMSE values generally increased with increasing object size. This lack of distinct differences in adjusted R^2 values among object sizes means that reducing lidar point spatial coverage had little effect on modeling attempts, with potential implications for a

more sampling-oriented approach to lidar-based forest inventories.

The lack of modeling differences across varying object sizes furthermore was attributed to the hierarchical nature of the segmentation algorithm, which resulted in small homogenous objects that served as building blocks for larger objects. Within-object homogeneity already was minimized at smaller average object sizes, resulting in no definitive difference in modeling results as object size increased through recombination of smaller objects. However, object-based modeling efforts were distinctly better than those found for existing, operational forest stands in the study area. This was attributed to the larger within-stand height variation in the case of existing stands when compared to the variation found within homogenous objects.

Modeling results were very promising, even though coniferous and combined adjusted R^2 values for volume and biomass were lower than those found in other published studies. Lower coniferous R^2 values were attributed in part to a smaller range of volume and biomass observed values, as well to the inherent variability found in Virginia Piedmont forests. Adjusted R^2 values for deciduous objects were higher than those found for a comparable, plot-level study in the same area. This result indicated that an object-level approach to deciduous volume and biomass modeling is a potential improvement over plot-based approaches. High R^2 values in the context of this study were unlikely, given that volume and biomass modeling were performed by using only height-related values. This was due to the nature of the modeled field data, which were based on diameter-at-breast-height (biomass) as well as height (volume). RMSE values compared favorably with those found in other distributional modeling studies. Low RMSE values indicated that models could find applicability in an operational context, even given low R^2 values.

Forward and Mallow's Cp selection proved successful in the reduction of independent variables from as many as 75 initial height distributional variables to the fewer than 10 used for final modeling. Further variable reduction through correlation analysis proved critical to the process of reducing variables. Final model selection from all candidate models was based on Mallow's Cp, adjusted R^2, RMSE values, and model simplicity. All criteria proved useful and even necessary to select a single best option from a large set of Mallow's Cp recombined variable models. Final variables spanned the whole spectrum of possibilities, from general mean and range height values to more abstract coefficient of variation and SD-type variables. Both regular and canopy cover percentiles also were well represented. The inclusion of intensity variables was interesting since few studies (Means et al. 1999, Brandtberg et al. 2003) have included intensity values as part of forest biophysical modeling. The wide range of selected variables indicated that sophisticated lidar scanners that can record multiple returns and intensity associated with each lidar hit might well be necessary for effective modeling of variation in more complex forests.

Per-object volume and biomass modeling has the potential of constituting part of a complete lidar-based inventory. Segmentation, volume and biomass modeling, and eventual object-oriented classification could form a cohesive approach to forest inventory using remote sensing data, specifically lidar technology. Segmentation of lidar-derived data has the benefit of establishing homogenous objects for subsequent volume and biomass modeling, resulting in scalable units that can be conglomerated along with all associated per-object estimates. A variable forest stand could thus be modeled at a more homogenous substand level. Although this was not investigated, it is possible that stand-level estimates will be more precise due to such a scalable, integrated approach. Additionally, limited fieldwork will be required for any given region. Potential fieldwork includes limited segmentation verification, establishment of volume-lidar distribution regression equations, and collection of forest type information. Established distributional volume and lidar equations could be applied for future stands and derived objects, with periodic verification using either fixed or variable plots. Models would have to be calibrated or even redeveloped for different regions, as it seems that results are geographically dependent (Means et al. 2000, Makela and Pekkarinen 2001, Næsset 2002, Pekkarinen 2002). Issues that potentially are critical to operational implementation include determination of the number of plots required for proper model fitting and the ideal object size for model development and application. The effect of variations in lidar technology, e.g., single versus multiple returns and the lack of intensity returns on most sensors, as well as aspects related to methodology, also need to be investigated. The lack of distinct differences in modeling results among object sizes has shown that a limited lidar point spatial coverage has significant potential in operational modeling of forest volume and biomass.

Literature Cited

AVERY, T.E., AND H.E. BURKHART. 1994. *Forest measurements*, 4th ed. McGraw-Hill, Boston, MA. 408 p.

BAATZ, M., AND A. SCHÄPE. 2000. Multiresolution segmentation—An optimization approach for high quality multi-scale image segmentation. P. 12–23 in *Angewandte Geographische Informationsverarbeitung* XII. Beiträge zum AGIT-Symposium Salzburg, September 2000, Strobl, J., T. Blaschke, and G. Griesebner (Hrsg.). Herbert Wichmann Verlag, Karlsruhe.

BRANDTBERG, T., T.A. WARNER, R.E. LANDENBERGER, AND J.B. MCGRAW. 2003. Detection and analysis of individual leaf-off tree crowns in small footprint, high sampling density lidar data from the eastern deciduous forest in North America. *Remote Sens. Environ.* 85(2003):290–303.

BURROUGH, P.A., AND R.A. MCDONNEL. 1998. *Principles of geographical information systems*. Oxford University Press, Oxford, UK. 333 p.

CLARK III, A., D.R. PHILLIPS, AND D.J. FREDERICK. 1986. *Weight, volume, and physical properties of major hardwood species in the Piedmont*. USDA Forest Service, Southeastern Forest Experiment Station Research Paper SE-255, June 1986.

DOUGLAS, T.E., D.L. EVANS, K.L. BELLI, AND S.D. ROBERTS.

2003. *Classification of pine and hardwood by the distribution and intensity of lidar returns.* ISPRS "Three dimensional mapping workshop from InSAR and LIDAR," June 17–19, 2003, Portland, Oregon. 5 p.

DRAKE, J.B., R.O. DUBAYAH, D.B. CLARK, R.G. KNOX, J.B. BLAIR, M.A. HOFTON, R.L. CHAZDON, J.F. WEISHAMPEL, AND S.D. PRINCE. 2002. Estimation of tropical forest structural characteristics using large-footprint lidar. *Remote Sens. Environ.* 79(2002):305–319.

DRAPER, N.R., AND H. SMITH, 1981. *Applied regression analysis,* 2nd ed. John Wiley and Sons, Inc., New York. 709 p.

ECOGNITION USER'S MANUAL. 2003. *Definiens imaging.* Available at *www.definiens.com*; last date of access Oct. 24, 2006.

ENGDAHL, M.E., J. PULLIAINEN, AND M. HALLIKAINEN. 2003. Combined land-cover classification and stem volume estimation using multitemporal ERS tandem INSAR data. In *Proc. of IGARSS 2003 IEEE*, July 21-25, 2003. Toulouse. IEEE International, Piscataway, NJ. 3 p.

HODGSON, M.E., J.R. JENSEN, L. SCHMIDT, S. SCHILL, AND B. DAVIS. 2003. An evaluation of LIDAR- and IFSAR-derived digital elevation models in leaf-on conditions with USGS Level 1 and Level 2 DEMs. *Remote Sens. Environ.* 84(2003):295–308.

KAYITAKIRE, F., C. FARCY, AND P. DEFOURNY. 2002. Ikonos-2 imagery potential for forest stands mapping. ForestSAT Symposium, Heriot Watt University, Edinburgh, August 5–9, 2002. 11 p.

KELLNDORFER, J.M., AND F.T. ULABY. 2003. Forest biomass inversion from SAR using object oriented image analysis techniques. In *Proc. of IGARSS 2003 IEEE*, July 21-25, 2003. Toulouse. IEEE International, Piscataway, NJ. 3 p.

KRESSLER, F., Y. KIM, AND K. STEINNOCHER. 2003. Object-oriented land cover classification of panchromatic KOMPSAT-1 and SPOT-5 data. In *Proc. of IGARSS 2003 IEEE*, July 21-25, 2003, Toulouse. IEEE International, Piscataway, NJ. 7 p.

LEFSKY, M.A., W.B. COHEN, S.A. ACKER, G.G. PARKER, T.A. SPIES, AND D. HARDING. 1999. Lidar remote sensing of the canopy structure and biophysical properties of Douglas-fir and western hemlock forests. *Remote Sens. Environ.* 70:339–361.

LEFSKY, M.A., W.B. COHEN, D.J. HARDING, G.G. PARKER, S.A. ACKER, AND S.T. GOWER. 2002b. Lidar remote sensing of above-ground biomass in three biomes. *Global Ecol. Biogeogr.* 11(2002):393–399.

LEFSKY, M.A., W.B. COHEN, G.G. PARKER, AND D.J. HARDING. 2002a. Lidar remote sensing for ecosystem studies. *Bioscience* 52(1):19–30.

LI, W., G.B. BENIE, D.C. HE, S. WANG, D. ZIOU, AND Q.H.J. GWYN.1999. Watershed-based hierarchical SAR image segmentation. *Int. J. Remote Sens.* 20(17):3377–3390.

MACLEAN, G.A., AND W.B. KRABILL. 1986. Gross-merchantable timber volume estimation using an airborne lidar system. *Can. J. Remote Sens.* 12(1):7–18.

MAGNUSSEN, S., AND P. BOUDEWYN. 1998. Derivations of stand heights from airborne laser scanner data with canopy-based quantile estimators. *Can. J. Forest Res.* 28:1016–1031.

MAKELA, H., AND A. PEKKARINEN. 2001. Estimation of timber volume at the sample plot level by means of image segmentation and Landsat TM imagery. *Remote Sens. Environ.* 77:66–75.

MEANS, J.E., S.A. ACKER, B.J. FITT, M. RENSLOW, L. EMERSON, AND C.J. HENDRIX. 2000. Predicting forest stand characteristics with airborne scanning lidar. *Photogramm. Eng. Remote Sens.* 66(11):1367–1371.

MEANS, J.E., S.A. ACKER, D.J. HARDING, J.B. BLAIR, M.A. LEFSKY, W.B. COHEN, M.E. HARMON, AND A. MCKEE. 1999. Use of large-footprint scanning airborne lidar to estimate forest stand characteristics in the western Cascades of Oregon. *Remote Sens. Environ.* 67:298–308.

MONTGOMERY, D.C., E.A. PECK, AND G.G. VINING, 2001. *Introduction to linear regression analysis,* 3rd ed. John Wiley and Sons, Inc., New York. 641 p.

NÆSSET, E. 2002. Predicting forest stand characteristics with airborne scanning laser using a practical two-stage procedure and field data. *Remote Sens. Environ.* 80(2002):88–99.

NELSON, R., W. KRABILL, AND J. TONELLI. 1988. Estimating forest biomass and volume using airborne laser data. *Remote Sens. Environ.* 24:247–267.

NILSSON, M. 1996. Estimation of tree heights and stand volume using an airborne lidar system. *Remote Sens. Environ.* 56:1–7.

NUGROHO, M., D.H. HOEKMAN, AND R. DE KOK. 2002a. *Analysis of the forests spatial structure using SAR and Ikonos data.* Presented at ForestSAT Symposium, Heriot Watt University, Edinburgh, August 5–9, 2002. 10 p.

NUGROHO, M., D.H. HOEKMAN, AND R. DE KOK. 2002b. *Analysis of forest spatial structure using spatial decision rule.* Presented at ForestSAT Symposium, Heriot Watt University, Edinburgh, August 5–9, 2002. 8 p.

PARRESOL, B.R. 1999. Assessing tree and stand biomass: A review with examples and critical comparisons. *For. Sci.* 45(4):573–593.

PEKKARINEN, A. 2002. Image segment-based spectral features in the estimation of timber volume. *Remote Sens. Environ.* 82:349–359.

POPESCU, S.C., R.H. WYNNE, AND R.F. NELSON. 2002. Estimating plot-level tree heights with lidar: Local filtering with a canopy-height based variable window size. *Comput. Electron. Agr.* 37(2002):71–95.

POPESCU, S.C., R.H. WYNNE, AND J.A. SCRIVANI. 2004. Fusion of small-footprint lidar and multispectral data to estimate plot-level volume and biomass in deciduous and pine forests in Virginia, U.S.A. *For. Sci.* 50(4):551–565.

RIAÑO, D., E. MEIERC, B. ALLGÖWERC, E. CHUVIECOA, AND S.L. USTIN. 2003. Modeling airborne laser scanning data for the spatial generation of critical forest parameters in fire behavior modeling. *Remote Sens. Environ.* 86(2003):177–186.

SAUCIER, R.J., AND A. CLARK III. 1985. *Tables for estimating total tree and product weight and volume of major southern tree species and species groups.* Southwide Energy Committee, American Pulpwood Association, Inc., Rockville, MD.

SCHROEDER, P., S. BROWN, J. MO, R. BIRDSEY, AND C. CIESZEW-SKI. 1997. Biomass estimation for temperate broadleaf forests of the United States using inventory data. *For. Sci.* 43:424–434.

SEIELSTAD, C.A., AND L.P. QUEEN. 2003. Using airborne laser altimetry to determine fuel models for estimating fire behavior. *J. For.* 101(4):10–15.

SHANDLEY, J., J. FRANKLIN, AND T. WHITE. 1996. Testing the Woodcock-Harward image segmentation algorithm in an area of southern California chaparral and woodland vegetation. *Int. J. Remote Sens.* 17(5):983–1004.

SHANKAR, B.U., C.A. MURTHY, AND S.K. PAL. 1998. A new gray level based Hough transform for region extraction: An application to IRS images. *Pattern Recogn. Lett.* 19(1998):197–204.

SHARMA, M., AND R.G. ODERWALD. 2001. Dimensionally compatible volume and taper equations. *Can. J. For. Res.* 31(5):797–803.